

Impact of Crystallographic Surface on the Planar Anisotropy of Tightening Reaction in 316 Stainless Steel Sheet

Ch. Mallikarjun¹, G. Bala Narsimha², S. Ramthulla³, T. Raja Santhosh³

Associate Professor, SMEC, Telangana, India.¹,

Assistant Professor, SMEC, Telangana, India.^{2,3}

ABSTRACT: The impact of crystallographic surface on planar anisotropy in strain and low cycle exhaustion was explored for tests machined along 0, 45 and 90° edge regarding the moving heading of hot rolled and tempered 316 stainless steel sheet utilizing electron backscatter diffraction. The ductile conduct of the three distinct introductions demonstrated little anisotropy. Nonetheless, the weakness life of tests got along rolling (0°) and transverse heading (90°) were comparable while the example along 45° to moving bearing indicated higher cyclic crawl rate (tightening) and least weariness life at various anxiety cycling parameters in stretch control mode. The anisotropic tightening conduct in SS 316 can be ascribed to operation of higher slip frameworks in the rolling and transverse examples with $\langle 100 \rangle$ surface while $\langle 101 \rangle$ surface along 45° specimen with confined slip. This adds to higher backstress and lower weariness life in the last mentioned. Likewise, disfigurement twinning that rules in 0 and 90° example in pressure gives unwinding of backstress amid cyclic stacking by detwinning which additionally adds to higher weakness life contrasted with 45° specimen.

I. INTRODUCTION

Anisotropy in mechanical properties is an inborn normal for metallic materials and has been contemplated broadly in monotonic load- ing [1] . In a polycrystalline material, anisotropy in plastic twisting conduct emerges because of particular introduction of grains or crystallo-realistic surface that controls the mechanical reaction of the example in monotonic stacking. This gets showed as far as various Young modulus, yield quality, extreme elasticity and pliability esteems for tests acquired along various bearings as for a settled course, say the moving heading, for a moved sheet of polycrystalline material. An intensive comprehension of impact of surface as far as an-isotropic in-plane tractable properties for moved sheets is set up but that in cyclic stacking is as yet unexplored. Single precious stones speak to the ex-treme instance of anisotropy and their monotonic conduct has been well archived for various face focus cubic (fcc) materials. In any case, cy-click disfigurement conduct of fcc single precious stones is not broadly inves-tigated. Li et al. examined cyclic misshapening conduct of fcc single gems of various introductions as an element of stacking shortcoming vitality (SFE). They demonstrated that there is an evolution of unmistakable disengagement sub-structure for diverse orientations of fcc single precious stone regardless of the SFE, which can be clarified on the premise of operation of various octa- hedral slip frameworks (essential, cross, conjugate and basic) for guaranteed introduction. This prompts agreeable marvel for separation pop- ulations and there is rivalry between their versatility and non-straight association like creation, destruction and sticking that adds to arrangement of particular inhomogeneous spatial examples of separations. It was watched that strain controlled low cycle weakness of $\langle 100 \rangle$ fcc single precious stone prompted the development of maze (two dimensional divider) sub-structure while veins (one dimensional) and cell dividers (three dimen-sional) were seen in $\langle 111 \rangle$ single precious stone. The $\langle 101 \rangle$ single precious stone that has predetermined number of slip frameworks (four) contrasted with $\langle 100 \rangle$ furthermore, $\langle 111 \rangle$ introduction (eight and six separately) demonstrated a substructure including diligent slip groups. Comparable separation substructures are likewise seen in push controlled tests with the cell structure dom- inating the microstructure because of higher estimation of aggregated plastic strain in the twisted specimens. The disengagement substructure framed under strain and stress control mode influences the cyclic solidifying/delicate ending reaction of the gem . For a polycrystalline

International Journal of Innovative Research in Science, Engineering and Technology

(An ISO 3297: 2007 Certified Organization)

Vol. 5, Issue 5, May 2016

material, comparable separation structures are seen in singular grains relying upon their introduction while keeping up strain similarity criteria with neighboring grains. Along these lines, it can be normal that crystallographic surface can influence the development of substructure in this way controlling the low cycle exhaustion life in anxiety control mode for polycrystalline tests.

The anxiety controlled cyclic misshapening can be unevenly professional portioned and non-relative. Exhaustion disappointment under unbalanced cyclic stacking in the flexible plastic administration is of extraordinary worry for stack bearing material in benefit. The nearness of annihilated leftover separations created because of halter kilter cyclic load drives to accumulation of plastic strain (known as tightening strain) toward mean worry in each cycle. The fatigue failure occurs when there meant separation civility is same as that in tractable example at a definitive elasticity .

Tightening conduct of modernly important interstitial free (IF) steel , 20MnMoNi55 steel , SA333 , 42CrMo steel and austenitic stainless steels like SS304 and SS316 have been extensively concentrated in the current past. Notwithstanding the previously mentioned ferrous combinations, non-ferrous metals and compounds have likewise been investigated. The association of exhaustion and tightening has been examined by Varvani et al. for uni axial and multi-hub stacking conditions. These investigations depend on the impact of stress cycle parameters (mean stress and stress plentifulness) on tightening reaction of materials. The general tightening reaction is described by a decline in weariness an existence with increment in stretch sufficiency or mean anxiety. It has been found that impact of stress plenty fullness is more articulated than mean anxiety on weariness life. Tightening strain and tightening strain rate have been observed to be an element of mean anxiety and rely upon cyclic solidifying/ cyclic softening conduct of the material. It is suggested that the measure of backstress increments with increment in mean anxiety prompting increment in the cyclic yield stretch that modifies the tightening strain accumulated in the material and therefore the weakness life . Ratcheting life has been found to increment with diminish in stretch amplitude and mean worry in the vast majority of the previously mentioned compounds aside from SS 304 steel. This odd conduct of SS 304 which indicates increment in tightening existence with increment in mean worry past a specific esteem was ascribed to the expansion in leftover disengagement thickness, arrangement of disfigurement instigated martensite and bigger separation cell measure in the substructure that empowered aggregation of more endure higher mean stretch .

In any case not very many examinations have been completed on an-isotropy in weariness conduct of materials except for few results on spring steel also, produced steel . The anisotropy in weariness quality in these materials has been credited to the morphology and introduction of oxides and sulfide considerations regarding the stacking bearing. A current report completed by Paul] has demonstrated the anisotropy in tightening conduct of body focus cubic IF steel twisting by pencil float. The impact of twinning which plays significant role in twisting of low stacking fault vitality fcc material and its in fluency on anisotropic conduct in tightening has not been considered however. In this manner, the investigation of tightening reaction and the basic miniaturized scale instruments as an element of introduction is required in low stacking fault vitality fcc material like stainless steel where octahedral slip what's more, twinning assume a prevailing part amid plastic disfigurement. Moreover, this examination will frame the premise to change the scientific plans gave by past specialists for estimation of tightening life in future .

Stainless steel (SS) 316 has been decided for exhibit examination which is a built up material for atomic weight vessels, steam turbines and different power apparatuses and is regularly presented to asymmetrically relative stacking amid benefit. In the present examination, three unique mixes of stress adequacy and mean anxiety have been connected on three unique (0, 45 and 90°) introduction of the stacking tomahawks as for moving course. The smaller scale systems of tightening conduct in distinctively arranged SS 316 specimens will be set up from the examination of microstructure and smaller scale surface utilizing electron backscatter diffraction (EBSD) procedure.

II. EXPERIMENTAL

Hot rolled and toughened 200 mm × 200 mm × 3 mm sheet of SS 316 steel were utilized to examine the impact of in-plane anisotropy in the introduce examination. Level examples of measurement following ASTM Standard E606 were machined from the sheet such that the stacking tomahawks of the examples were making an edge of 0, 45 and 90° to the moving bearing. Fig. 1 an and b indicate schematic of various orientations and example measurements individually. Every one of the investigations were directed on the above examples at room temperature utilizing BiSSNano Plug " n " Play servo-pressure driven universal test machine of 25KN limit. Elastic tests were done on the above examples at steady strain rate of $5 \times 10^{-2} \text{ s}^{-1}$ to acquire mechanical properties of the material. Building stress controlled uni

International Journal of Innovative Research in Science, Engineering and Technology

(An ISO 3297: 2007 Certified Organization)

Vol. 5, Issue 5, May 2016

axial uneven anxiety cycling was forced on the examples. The test parameters were chosen in light of the work completed by Kang et al. Diverse mix of stress sufficiency/yield push (σ_a / σ_y) furthermore, mean anxiety/yield push (σ_m / σ_y) proportion are given in Table 1 . A sinusoidal waveform was utilized to play out the tests and the cyclic recurrence was kept at 0.5 Hz for every one of the tests. Tests were proceeded till disappointment and push – strain information gained all through the test to get 200 information focuses per push cycle. Tests were led under programming control running on a PC interfaced to the control arrangement of the testing machine. The as-got material was separated at mid-thickness and cleaned before subjecting it to mass surface estimation. Mass texture was decided on RigakuUltima X-beam diffract meter fitted with a surface goniometry using Co K α radiation in Schulz re flections geometry.

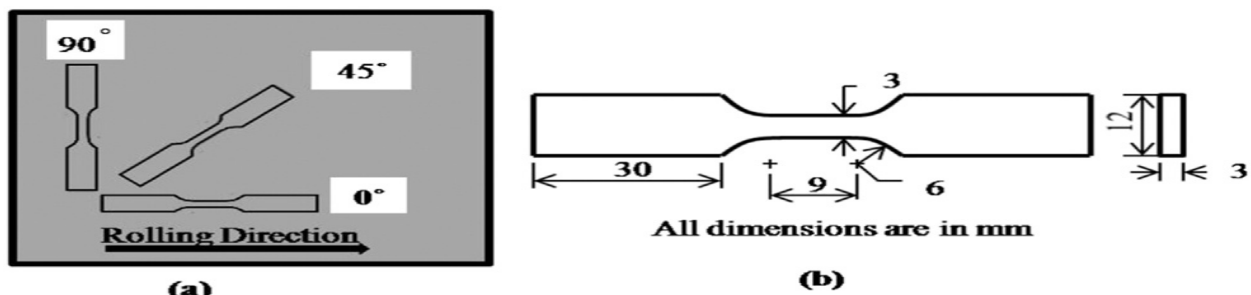


Fig. 1. (a) Schematic of different specimen orientations (b) E-606 standard specimen dimension.

Three inadequate (111), (200) and (220) shaft figures were resolved in a 5° by 5° framework. The information got from these post figures were utilized to ascertain the total introduction dissemination work (ODF) utilizing Reseat programming and finish shaft figures have been created. The mass surface information was discretized to 2000 single introductions utilizing Resmat programming to anticipate Lankford Coef ficient (r) for 0 – 90° edge of stacking pivot to moving bearing utilizing viscoplastic self-consistent (VPSC) gem versatility demonstrate VPSC-7 . Correspondingly Taylor factor was resolved for octahedral slip and blend of octahedral slip and twinning utilizing MTM-TAY programming. The tried examples near crack area was electropolished utilizing A3 electrolyte and at that point subjected to miniaturized scale surface examination utilizing a field-outflow firearm filtering electron magnifying lens (JSM-7100F FE-SEM) fitted with Ox- passage Channel 5 electron back disperse diffraction (EBSD) connection. An range of 400 × 400 μm^2 was checked with a stage size of 0.5 μm . Fractographs of the tried specimens were taken utilizing JEOL Tungsten fi lament filtering electron magnifying lens.

Table-1 Stress parameters used for asymmetric cyclic loading.

Combination	σ_a/σ_y	σ_m/σ_y
I	1.1	0.4
ii	1.2	0.4
iii	1.2	0.5

III. RESULTS

1.Initial material :

The microstructure of as got hot rolled and strengthened sheet appeared in Fig. 2a demonstrates nearness of tempering twins inside austenite grains. (111) and (220) shaft figures appeared in Fig. 2b uncover a run of the mill Metal Goss sort surface with a solid Goss {110} <001> part in the steel sheet. The reverse shaft figures along RD appeared in Fig. 2c portrays arrangement of <001> bearing along the moving course while the ND converse shaft figure demonstrates a solid <110> segment. The surface in the moved sheet is depicted regarding converse shaft figure as uniaxial distortion was done in weariness. Along these lines it is surmised that the 0 and 90° specimens have a solid <100> fiber surface

with minor $\langle 111 \rangle$ segment along the ductile pivot while the 45° specimen has a solid $\langle 110 \rangle$ surface along the ductile pivot.

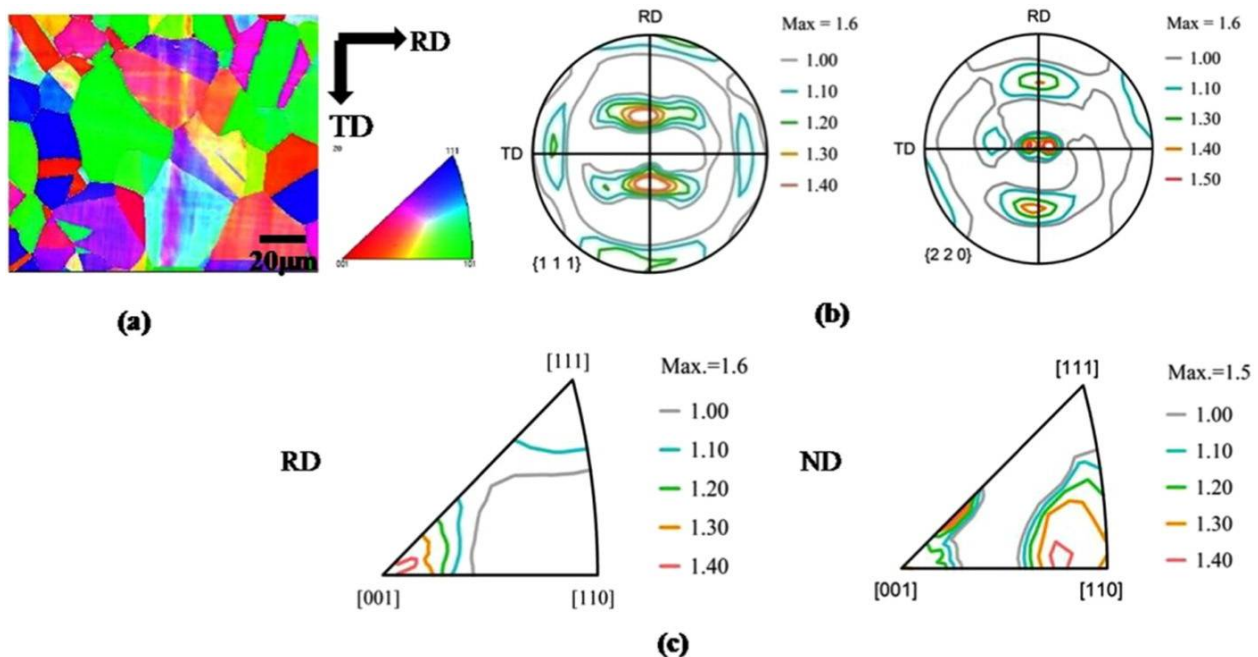


Fig. 2. (a) Crystal orientation map from EBSD (b) $\langle 111 \rangle$ and $\langle 220 \rangle$ pole figures (c) inverse pole figure maps along RD and ND from bulk texture measurement in hot rolled and annealed SS316.

2. Effect of sample orientation on tensile properties of SS 316 steel

The genuine anxiety genuine strain plot as an element of three distinct introductions regarding moving course is appeared in Fig. 3. The measured tractable properties detailed in Table 2 indicates anisotropy in ductile conduct as a component of introduction. The yield quality (YS) was higher for the 45° introduction contrasted with the 0 and 90° example while a definitive elasticity (UTS) was bring down for the previous contrasted with the last two specimens. The strain solidifying coefficient (n) of the 0 and 90° specimen is higher contrasted with the 45° introduction showing lower malleability of this introduction. The computed estimations of Taylor factor utilizing octahedral slip and slip + twinning show unimportant contrast for three diverse introduction. The degree of plastic anisotropy of the material has been evaluated from Lankford co-effective. The Lankford co-effective (r) which is the proportion of plastic strain along transverse bearing (TD) to typical bearing (ND) as given in Eq. (1).

$$R = \epsilon_{TD} / \epsilon_{ND} \text{-----(1)}$$

The variety of Lankford co-proficient, r with moving course (Fig. 4) unmistakably demonstrates planar plastic anisotropy of the material with least r-esteem along moving heading and most extreme at a point of 45° to moving heading which is reflected in the malleable property as announced prior. Because of the comparative mechanical conduct of 0 and 90° introductions, from this time forward we will consider just two unmistakable introduction 0° and 45° test for facilitate investigation.

3. Effect of sample orientation on ratcheting

The cyclic anxiety strain bend for a specific anxiety a abundance mean push mix for 150 cycles appeared in Fig. 5 uncovers that aggregated strain is bigger in 0° test contrasted with 45° introduction for the same number of cycles. The degree of cover between successive hysteresis circles demonstrate that the width (plastic strain sufficiency) of each hysteresis circle in 0° test is bigger contrasted with 45° introduction. The bend appeared in Fig. 6a portrays that for same σ_a/σ_y and σ_m/σ_y add up to gathered tightening

International Journal of Innovative Research in Science, Engineering and Technology

(An ISO 3297: 2007 Certified Organization)

Vol. 5, Issue 5, May 2016

strain in 45° introduction is bring down analyzed to different introductions and shows early disappointment. The aggregated tightening strain in each cycle is ascertained in view of Eq. (2):

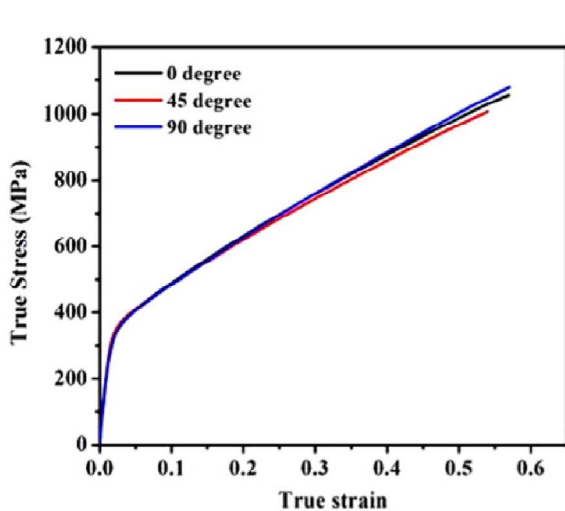


Fig. 3. True stress-true strain as a function of orientation of tensile axis with respect to rolling direction

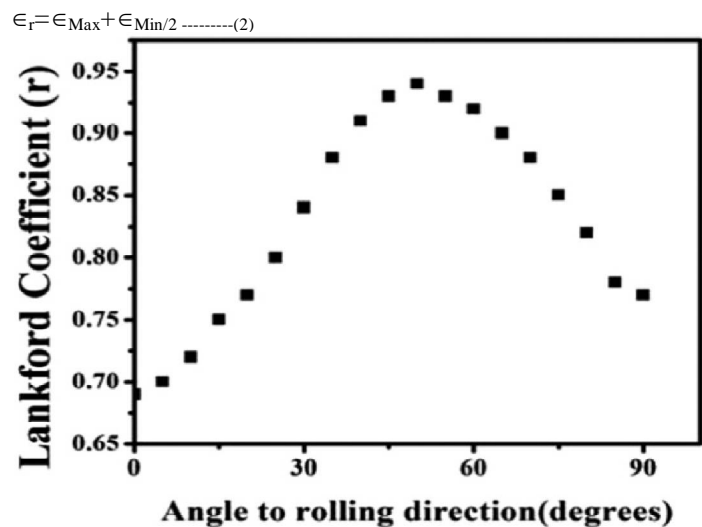


Fig. 4. Variation of Lankford Coefficient as a function of angle to rolling direction.

The quantity of cycles to disappointment is plotted in Fig. 6b for various blends of (σ_a/σ_y) and (σ_m/σ_y) proportion at three unique introductions. It demonstrates that for a specific anxiety abundance mean anxiety blend number of cycles to disappointment in 45° example is a large portion of the quantity of cycles to disappointment got in the 0° introduction. At consistent mean anxiety, cycles to disappointment diminish for every one of the specimens with increment in push adequacy. In any case, at steady anxiety a abundance, the quantities of cycles to disappointment diminish for 0 and 90° specimen yet increment for 45° introduction with increment in mean anxiety.

The enduring state sneak rate figured in Table 3 demonstrates that 45° specimen has higher enduring state crawl rate than 0 and 90° introductions for two distinctive σ_a/σ_y proportion and the crawl rate is higher for 45° specimen at bring down anxiety abundance.

The varieties in cyclic crawl rate (der/dN) with increment in number of cycles (upto 500 cycles) for two distinctive σ_a/σ_y , at consistent σ_m/σ_y are introduced in Fig. 7a and b separately. The outcomes in these figures show that der/dN diminishes with expanding number of cycles. The lessening in der/dN is quick up to around ten cycles, after which the change in the size of der/dN is little and it turns out to be practically steady after around 200 cycles. This demonstrates the amassing of tightening strain in the underlying few cycles is fast trailed by fulfillment of a consistent state crawl rate esteem.

4. Evolution of microstructure and micro-texture:

The microstructure and small scale surface from surface near the break district of the pliable test example for 0 and 45° introductions are appeared in Fig. 8a. It demonstrates that grains having introduction near $\langle 001 \rangle \parallel LA$ (red) accommodate maximum strain by separation glide where as $\langle 111 \rangle \parallel LA$ (blue) grains are were essentially reoriented because of twinning prompting the improvement of solid surface after twisting. The twin morphology is thicker in 0° contrasted with 45° introduction. Grain limit character dissemination given in Table 4 shows the

nearness of $\Sigma 3$ correspondent site cross section limits (CSL) that compares to twin in fcc materials. The elastic tried examples are portrayed by the nearness of high portion of low edge grain limits while noteworthy $\Sigma 3$ limits demonstrate nearness of twinning in both the tests. BSD information can be utilized to assess the advancement of inter granular what's more, intragranular worry in an indirect manner by figuring extraordinary misorientation parameters [31]. The neighborhood normal misorientation (LAM) dissemination (Fig. 8b) for the ductile tried specimens demonstrate development of higher LAM for the 45° example demonstrating higher disengagement thickness and intragranular worry than the 0° test. The strain forming map for the two specimens delineated in Fig. 8c additionally appears higher strain for the 45° example demonstrating higher intergranular stretch in the 45° specimen contrasted with 0° test in pressure.

The disfigured microstructure and miniaturized scale surface acquired from surface near the break locale of the exhaustion tried example are appeared in Fig. 9a for 0 and 45° introductions. The microstructure uncovers volume division of twin lamella is higher in 0° introduction and the sky is the limit from there grain fracture is seen in 45° introduction. The morphology of the twin lamella is

International Journal of Innovative Research in Science, Engineering and Technology

(An ISO 3297: 2007 Certified Organization)

Vol. 5, Issue 5, May 2016

observed to be more slender in 0° introduction contrasted with 45° in spite of that saw after elastic disfigurement. The pattern in advancement of neighborhood normal misorientation is likewise switched in the cyclic stacking with the 0° test indicating higher LAM an incentive than the 45° test as saw from Fig. 9b. The strain form maps appeared in Fig. 9c relating to 0 and 45° introduction additionally delineates that 0° introduction can suit more strain contrasted with 45° introduction earlier to disappointment.

Fig. 10a and b demonstrate the GROD (grain reference introduction deviation) which is misorientation between the introduction of person pixel and the normal introduction of a similar grain for the 0 and 45° tests at disappointment in strain and cyclic stacking separately. The GROD maps unmistakably show that the deviation in introduction is higher for the consistently disfigured example contrasted with the ductile tried example. Essentially, higher misorientation is watched for the 0° test thought about to 45° specimen in strain. The grain limit misorientation conveyance detailed in Table 4 shows a special finding. The consistently tried tests are portrayed by a high division of exceptionally lowangle grain limits which is a reasonable sign of dynamic recuperation. The degree of dynamic recuperation is higher for the cyclic distorted examples analyzed to the malleable examples. It is to bementioned here that in monotonic stacking, there is a progressive increment in disengagement thickness with strain which adds to increment in part of low point grain limits at low to medium strain as saw in a malleable test. At higher strain, there is transformation of low edge grain limits to high edge grain limits prompting grain refinement in extreme plastic distortion forms. In any case, for the cyclic stacking, there is huge increment in part of low point grain limits that can be ascribed to arrangement of disengagement substructures like steady slip groups, maze furthermore, cell divider structure that has been accounted for in cyclic stressed tests in TEM. The disengagement thickness maps appeared in Fig. 11 acquired from ATOM programming [32] likewise show development of high disengagement thickness and lowdis location thickness locales for the malleable and cyclic twisted tests. It is watched that the cyclic disfigured examples have higher separation thickness contrasted with pliable tried example for a given introduction. It is additionally watched that the cyclic tried 0° test has higher separation thickness than the 45° specimen.

Table 2 Tensile property for three different orientations

Orientation	YS (MPa)	UTS (MPa)	% El n	UTS/YS	Mslip	Mslip+twin
0°	302.4± 5.3	595.8± 4.5	57 0.39	4 1.97	3.06	2.95
45°	317.9 ± 7.4	583.2 ± 8.2	54 0.373	1.83	3.05	2.96
90°	307.6 ± 3.5	600.1 ± 5.7	59 0.402	1.95	3.06	2.95

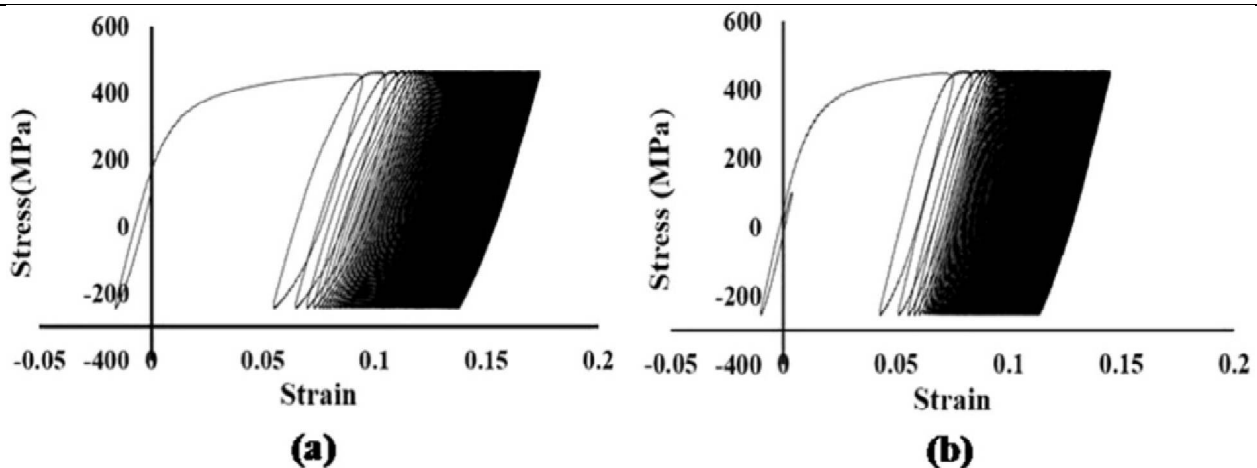


Fig. 5. Cyclic stress-strain curves for asymmetric loading condition of $\sigma_a/\sigma_y = 1.2$ and $\sigma_m/\sigma_y = 0.4$ (a) 0 degree and (b) 45°.

The relating crack surface appeared in Fig. 12a uncovers nearness of dimples and microvoids which are trademark bendable crack include yet both the elements are observed to be generally coarser in 45° contrasted with 0° introduction showing less pliability of 45° introduction. The relating crack surface appeared in Fig. 12b uncovers extraordinary weariness split start site in 0° 45° introduction. It is plainly watched that the 0° test demonstrates a higher portion of range indicating exhaustion break evelopment contrasted with 45° example. Like malleable specimens, the size of dimples in 45° specimens are coarser contrasted with the 0° test.

International Journal of Innovative Research in Science, Engineering and Technology

(An ISO 3297: 2007 Certified Organization)

Vol. 5, Issue 5, May 2016

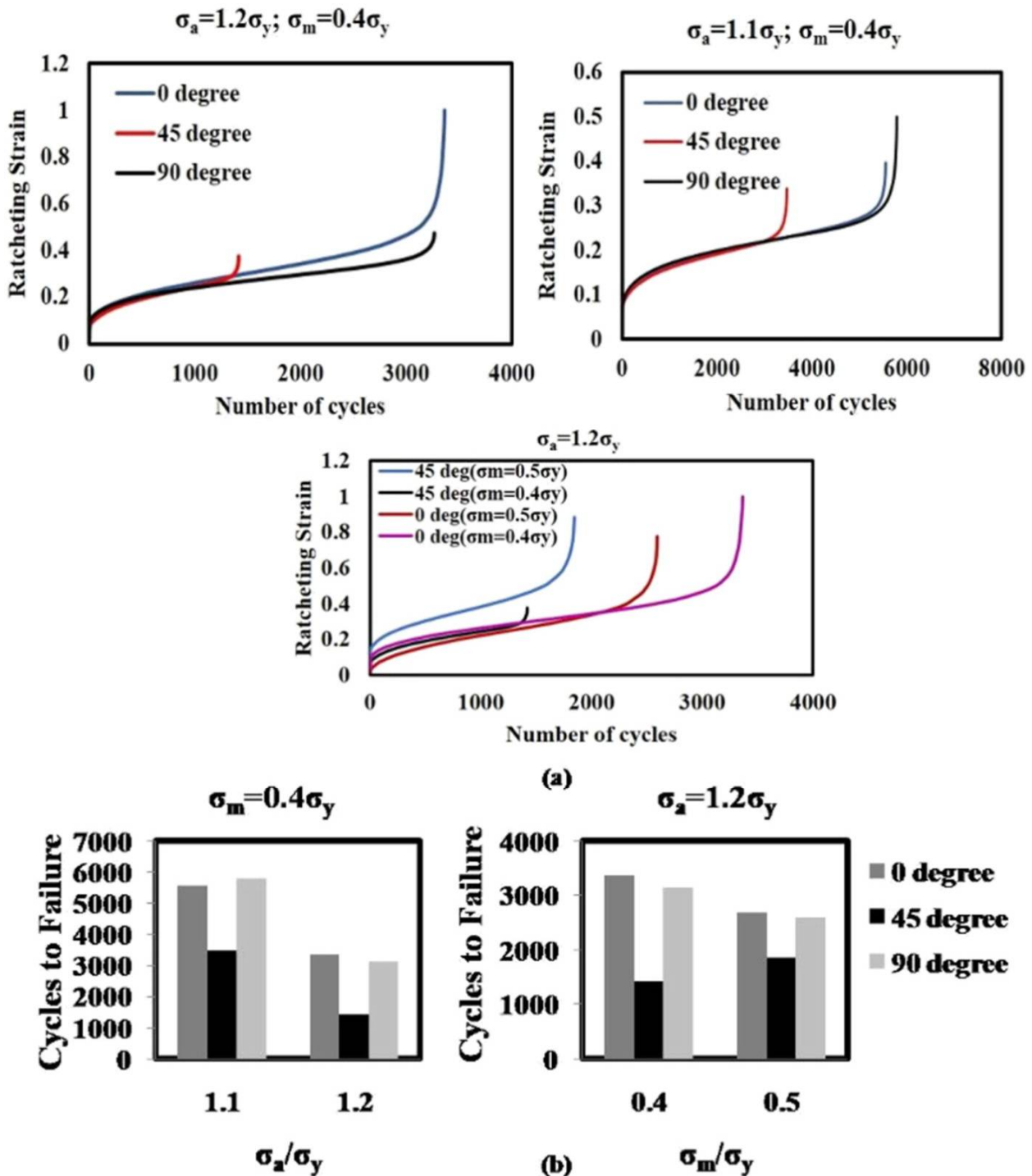


Fig. 6. (a) Evolution of ratcheting strain as a function of number of cycles for different orientations and (b) Bar chart showing number of cycles to failure as a function of different stress amplitude and mean stress.

International Journal of Innovative Research in Science, Engineering and Technology

(An ISO 3297: 2007 Certified Organization)

Vol. 5, Issue 5, May 2016

Table 3 Steady state creep rate at different loading parameters.

Orientation	Creep rate (s ⁻¹) @ $\sigma_a/\sigma_y = 1.2$	Creep rate (s ⁻¹) @ $\sigma_a/\sigma_y = 1.1$
0°	4×10^{-5}	2×10^{-5}
45°	5×10^{-5}	4×10^{-5}
90°	3×10^{-5}	2×10^{-5}

5. Anisotropy in tensile properties

Amid uniaxial malleable stacking in SS 316, disfigurement happens by slip at bring down strain took after by the arrangement of disfigurement twins at higher strain like SS 304 [33] and TWIP (Twin Induced Plasticity) steel [34]. With a specific end goal to clarify the lower yield quality (YS) in 0° introduction contrasted with 45° as saw from Fig. 3, Taylor factor was resolved from the underlying surface as the yield quality is straightforwardly corresponding to the Taylor factor

where τ_{CRSS} is basic settled shear stretch, $d\gamma_i$ is infinitesimal shear on a slip framework "i" and $d\epsilon$ is the forced strain, and $\langle M \rangle$ is the normal Taylor factor that gives the normal perviousness to plastic disfigurement by octahedral slip. Subsequently, introduction having higher Taylor factor ought to give higher yield quality. As saw from Table 2, Taylor factor decided utilizing octahedral slip system alone has insignificant distinction. Indeed, even in the wake of joining twinning there is immaterial contrast in Taylor factor which is additionally reflected in little distinction in YS of around 10–15MPa in the vicinity of 0 and 45° introduction and thus can't clarify higher YS in 45° introduction. In such a situation, higher YS in 45° introduction can be clarified on the premise of lower penchant of twinning. This is moreover basic from the perception that 45° introduction has more slender twins after malleable misshapening as twinning is less great. It is realized that twinning is agent even under versatile stacking and it is suggested that higher division of twins in 0 and 90° prompt lower YS.

Past yield worry as strain expands, the thickness of disengagements increment quickly which expands connection between portable disengagements coming about because of simple float at bring down strain and limits encourage distortion by slip. At higher strain, twinning action supports advance distortion process however in the meantime it changes over some of these glissile disengagements into sessile separations by changing the introduction of the twinned area and furthermore diminishes starting grain size which builds stretch required for further deformation by slip and formation of new twins [35]. This results in an increase in the work-hardening rate thus enhancing tensile strength and ductility [36]. The flow stress beyond yield stress is given by Eq. (4).

$$\sigma_f = \sigma_0 + \langle M \rangle \alpha G b \rho^{0.5} \text{ -----4}$$

where σ_f is the flow stress, σ_0 is friction stress, $\langle M \rangle$ average Taylor factor, α is a constant, G is shear modulus, b is burger vector and ρ is dislocation density in case slip is the sole mode of deformation.

Be that as it may, bring down LAM esteem and the separation thickness maps for ductile tried example shows bring down separation thickness for 0° introduction. Thus, higher extreme rigidity (UTS) of 0° introduction looked at to 45° is ascribed to higher strain solidifying because of development of thicker twins in 0° introduction contrasted with 45° introduction demonstrating simplicity of twin development in 0° introduction. Likewise higher estimation of GROD is an sign of initiation of numerous slip framework [37]. This clarifies the bring down UTS for 45° introduction contrasted with 0° test because of lower penchant for twinning in the previous. The higher penchant for twinning prompting bringing down of aggregate disengagement thickness in the austenite stage can be bolstered from the consequences of portrayal of separations after misshapening by Dutta et al. [38]. The fractographs appeared in Fig. 9 uncovers that in 0° introduction the voids shaped are littler in measure looked at to 45° introduction showing higher flexibility in 0° introduction. It brought about higher UTS/YS proportion in 0° contrasted with 45° introduction. This conduct has huge significance in tightening reaction amid deviated stacking in the versatile plastic administration clarified in next content

Role of slip in cyclic creep

Cyclic crawl rate is administered by two contending marvels [6]: cyclic solidifying reaction of the material and softening. Cyclic solidifying emerging from increment in disengagement thickness and its collaboration producing back stress which builds the anxiety required to defeat separation communication. The softening term consolidates softening

International Journal of Innovative Research in Science, Engineering and Technology

(An ISO 3297: 2007 Certified Organization)

Vol. 5, Issue 5, May 2016

due to destruction of separations and geometric softening because of increment in genuine worry under controlled designing anxiety cycling condition. In essential furthermore, auxiliary phase of crawl bend the commitment of geometric softening is little and it commands predominantly in tertiary stage. In this manner crawl rate is represented by rate of increment in back stress because of increment in disengagement thickness and the rate of back stress unwinding by twinning and disintegration of disengagement cell structure. In the essential locale back stress unwinding happens by twinning while back stress unwinding by obliteration of disengagement through cross slip happens in the optional consistent state locale after immersion of disengagement thickness and twin immersion.

Effect of twinning

Under the connected anxiety cycle parameters the material is subjected to organize I-II strain solidifying administration [41] of the genuine stress– genuine strain bend where both disengagement slip (single + different) and twin modes of disfigurement are dynamic. Due to the work-solidifying nature of the material in arrange II, the connected controlled anxiety is deficient for its required plastic misshapening and it produces backstress in the material. As indicated by Feau gas [41] produced back stress (χ) is parceled between intragranular highlights like disengagement cell divider (χ_w) and intergranular highlights like twin limits (χ_t) and grain limit (χ_b) framed during monotonic twisting. At bring down strain when disfigurement is limited locally within singular grains and planar slip administers the disfigurement procedure, at that point χ_w gives the real commitment to back stress. At higher strain when progress from planar to wavy slip happens and distortion happens all around, back stress is commanded by commitment from dislocations heaped up at twin and grain limits what's more, is specifically relative to disengagement thickness. So also amid tightening, at first as number of cycles expands the commitment from (χ_w) increments. Be that as it may, because of twinning a piece of the glissile disengagements are changed over to sessile separations inside the twinned locale.

This aides in decreasing the measure of backstress χ_w produced by lessening the aggregate number of glissile disengagements. Then again, amid switch stacking the backstress created because of remainder glissile disengagements help simple switch slip and the back stress created at the twin limit amid switch stacking get casual by the diminishing of twin lamella (detwinning), and this advance stressing of the surrounding matrix under the connected load. Comparable wonder of stress unwinding by diminishing of twinned area has been said before by a few scientists in Mg [42] and TWIP steel [43]. This causes diminish in crawl rate for introductory 50– 100 cycles. As the relative action of slip and twin system is a component of introduction of the grain with regard to stacking pivot, thus convenience of back stress is likewise unique in an unexpected way situated grains. It has been as of now talked about in Section 4.1 that at connected greatest anxiety, 0° introduction has low disengagement movement in any case, high twinning affinity contrasted with 45° introduction. Along these lines, (χ_w) 0° b (χ_w) 45° . So the rate of increment of back stress will be more in 45° contrasted with 0° bringing about more reduction in sneak rate in previous contrasted with last in the essential locale of crawl bend. As number of cycles expands (N100 cycles), χ_w begins diminishing because of immersion of separation thickness and the procedure of disintegration of disengagement cell proceeds. In this way past 100 cycles enduring state crawl rate is accomplished because of harmony between the rate of increment in back stress and rate of backstress unwinding. Be that as it may, because of limited slip in 45° introduction thickness of glissile disengagements turns out to be too low to maintain connected controlled worry by disengagement coast in the austenite grain framework or by twinning which is likewise very limited in this introduction. Along these lines, in the wake of coming to the unfaltering state administration of the crawl bend it bombs quickly demonstrating low weariness life.

IV. DETERMINATION OF RATCHETING STRAIN

Under the connected anxiety cycle parameters the material is subjected to organize I-II strain solidifying administration [41] of the genuine stress– genuine strain bend where both disengagement slip (single + different) and twin modes of disfigurement are dynamic. Due to the work-solidifying nature of the material in arrange II, the connected controlled anxiety is deficient for its required plastic misshapening and it produces back stress in the material. As indicated by Feaugas [41] produced back stress (χ) is parceled between intragranular highlights like disengagement cell divider (χ_w) and intergranular highlights like twin limits (χ_t) and grain limit (χ_b) framed during monotonic twisting. At bring down strain when disfigurement is limited locally within singular grains and planar slip administers the disfigurement procedure, at that point χ_w gives the real commitment to backstress. At higher strain when progress from planar to wavy slip happens and distortion happens all around, backstress is commanded by commitment from dislocations

International Journal of Innovative Research in Science, Engineering and Technology

(An ISO 3297: 2007 Certified Organization)

Vol. 5, Issue 5, May 2016

heaped up at twin and grain limits what's more, is specifically relative to disengagement thickness. So also amid tightening, at first as number of cycles expands the commitment from (χ_w) increments. Be that as it may, because of twinning a piece of the glissile disengagements are changed over to sessile separations inside the twinned locale. This aides in decreasing the measure of backstress χ_w produced by lessening the aggregate number of glissile disengagements. Then again, amid switch stacking the backstress created because of remainder glissile disengagements help simple switch slip and the backstress created at the twin limit amid switch stacking get casual by the diminishing of twin lamella (detwinning), and this advance stressing of the surrounding matrix under the connected load. Comparable wonder of stress unwinding by diminishing of twinned area has been said before by a few scientists in Mg [42] and TWIP steel [43]. This causes diminish in crawl rate for introductory 50– 100 cycles. As the relative action of slip and twin system is a component of introduction of the grain with regard to stacking pivot, thus convenience of backstress is likewise unique in an unexpected way situated grains. It has been as of now talked about in Section 4.1 that at connected greatest anxiety, 0° introduction has low disengagement movement in any case, high twinning affinity contrasted with 45° introduction. Along these lines, (χ_w) 0° b (χ_w) 45° . So the rate of increment of backstress will be more in 45° contrasted with 0° bringing about more reduction in sneak rate in previous contrasted with last in the essential locale of crawl bend. As number of cycles expands (N100 cycles), χ_w begins diminishing because of immersion of separation thickness and the procedure of disintegration of disengagement cell proceeds. In this way past 100 cycles enduring state crawl rate is accomplished because of harmony between the rate of increment in backstress and rate of backstress unwinding. Be that as it may, because of limited slip in 45° introduction thickness of glissile disengagements turns out to be too low to maintain connected controlled worry by disengagement coast in the austenite grain framework or by twinning which is likewise very limited in this introduction. Along these lines, in the wake of coming to the unfaltering state administration of the crawl bend it bombs quickly demonstrating low weariness life.

V. CONCLUSIONS

In plane anisotropy of SS 316 showed as far as various elastic quality and malleability on test along RD and TD on one hand and 45° test was enhanced amid unevenly relative cyclic stacking. It has been discovered that in SS 316, for a specific blend of unevenly relative cyclic stacking parameter introduction with most extreme Lankford Coefficient (i.e, 45°) demonstrated most astounding cyclic crawl rate and weakness life gets nearly split. In 0 and 90° introduction due to broad different slip the created separation thickness is higher and the required disengagement thickness to proceed with twisting procedure is kept up by ease back rate of planar to wavy slip change. On the other hand, limited slip and fast planar to wavy slip change prompts collection of high back worry in 45° specimen. Additionally, the nearness of twinning guides in unwinding of back stress in every one of the specimens and guarantee that impact of introduction is curbed thought about to materials where distortion happens just by slip.

International Journal of Innovative Research in Science, Engineering and Technology

(An ISO 3297: 2007 Certified Organization)

Vol. 5, Issue 5, May 2016

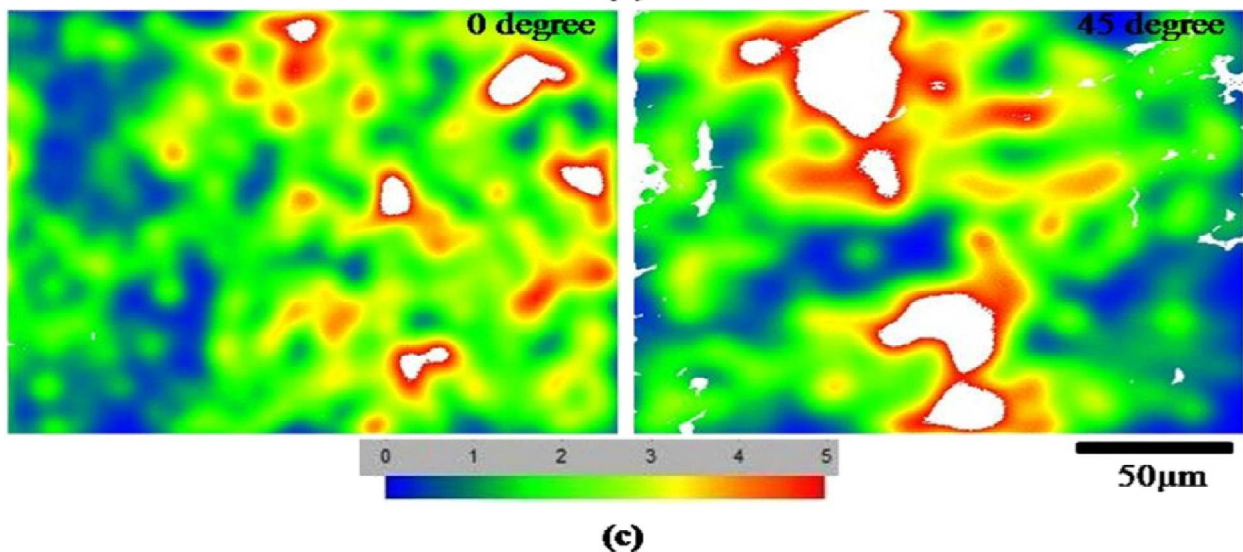
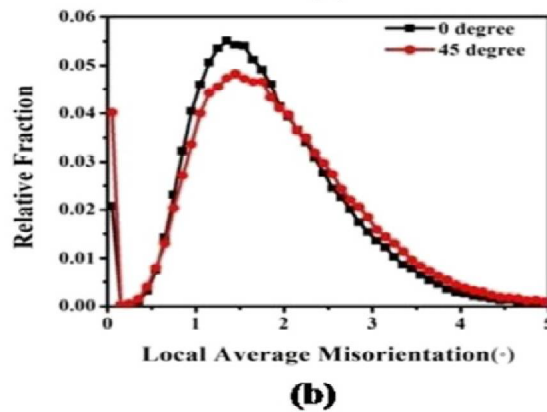
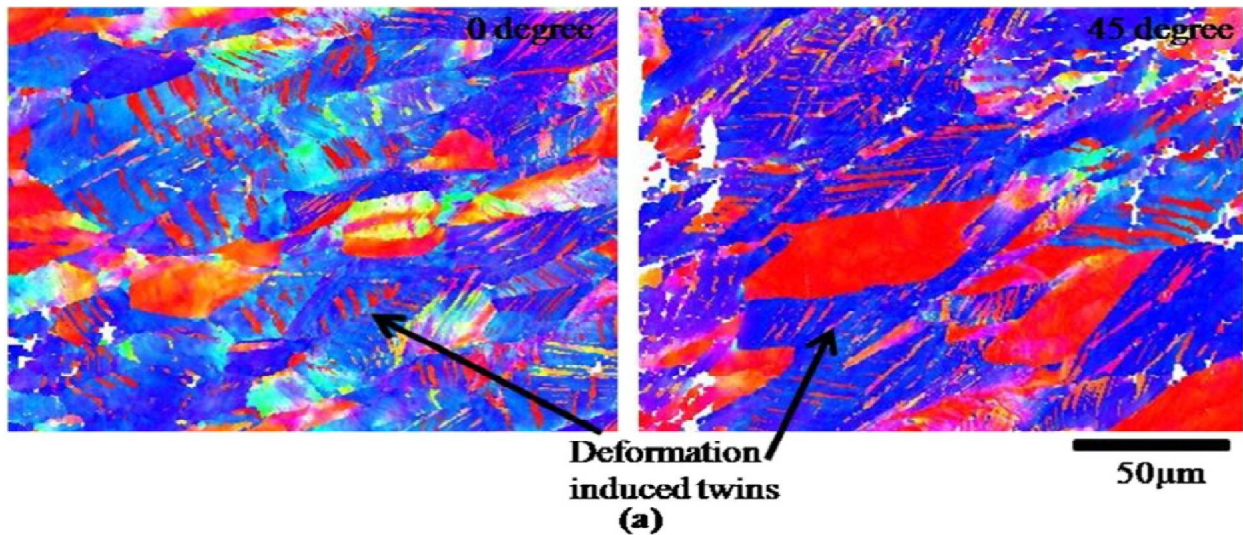


Fig. 8. (a) Crystal orientation maps along tensile direction (b) local average misorientation distribution and (c) Strain Contour maps for 0 and 45° orientation of SS 316 tensile specimen.

International Journal of Innovative Research in Science, Engineering and Technology

(An ISO 3297: 2007 Certified Organization)

Vol. 5, Issue 5, May 2016

(For interpretation of the references to color in this figure, the reader is referred to the web version of this article.)

Table 4
Evolution of grain Boundaries and misorientation in tensile and fatigue tested samples.

Orientation	%VLGB(2-5°)	%LAGB(5-15°)	%HAGB(15-60°)	(%) twin boundary	LAM°	GROD°
0°-tensile	59	8	33	5.8	1.80	0.404
45°-tensile	61	11	28	8.2	1.87	0.421
0°-fatigue	75	6.7	18.3	7.5	1.92	0.520
45°-fatigue	74	6.6	19.4	6.1	1.81	0.511

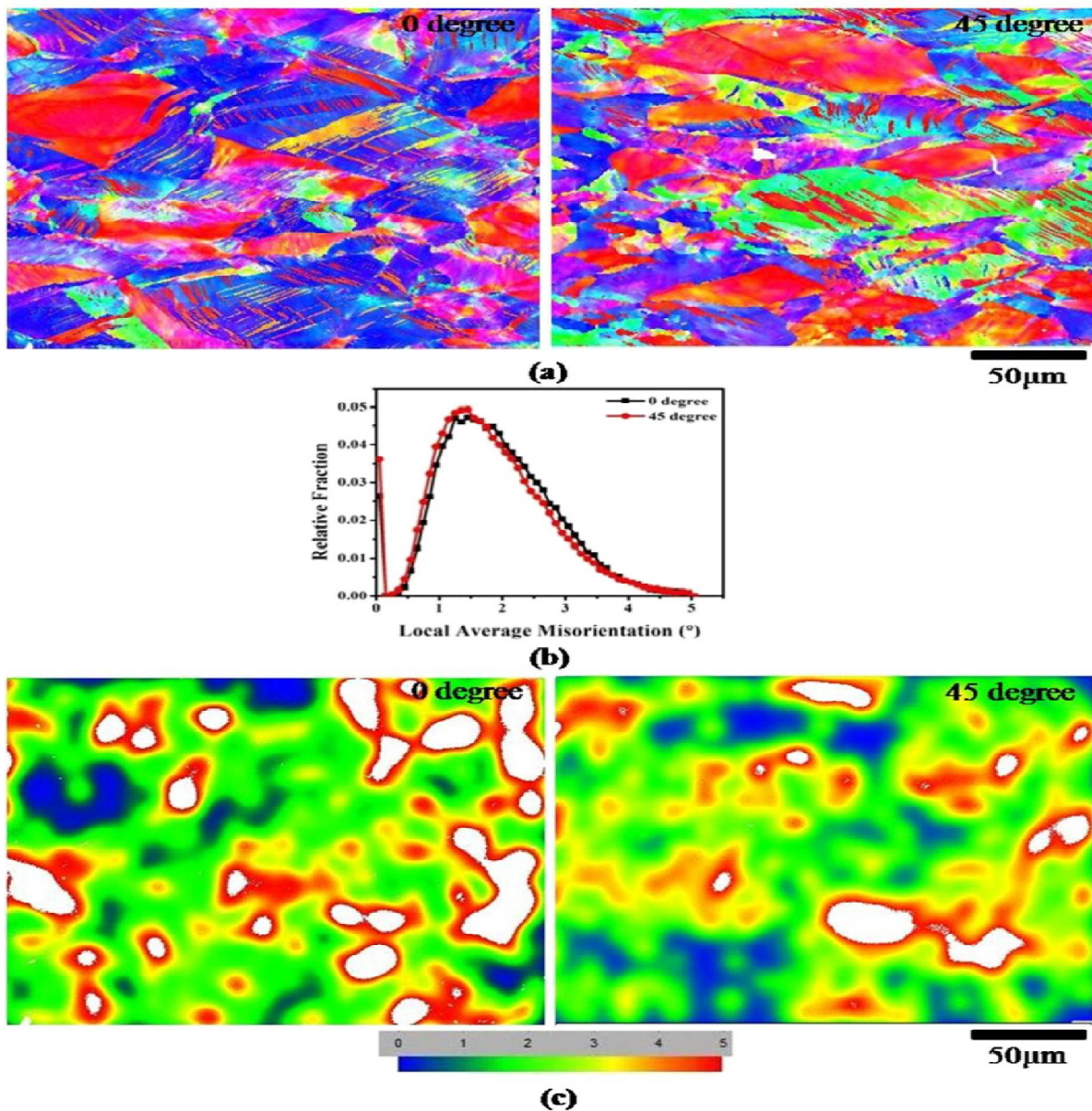


Fig. 9. (a) Crystal orientation maps along cyclic loading direction (b) local average misorientation distribution and (c) Strain contour maps for 0 and 45° orientation under asymmetric loading condition of $\sigma_a=1.2\sigma_y$ and $\sigma_m=0.4\sigma_y$.

International Journal of Innovative Research in Science, Engineering and Technology

(An ISO 3297: 2007 Certified Organization)

Vol. 5, Issue 5, May 2016

REFERENCES

- [1] U.F. Kocks, C.N. Tomé, H.R. Wenk, Texture and Anisotropy: Preferred Orientations in Polycrystals and Their effect on Materials Properties, Cambridge University Press, Cambridge, U.K., 1998
- [2] P. Li, S.X. Li, Z.G. Wang, Z.F. Zhang, Fundamental factors on formation mechanism of dislocation arrangements in cyclically deformed fcc single crystals, Prog. Mater. Sci. 56 (2011) 328–377.
- [3] T. Hassan, S. Kyriakides, Ratcheting in cyclic plasticity, part I: uniaxial behavior, Int. J. Plast. 8 (1992) 91–116.
- [4] K. Dutta, K.K. Ray, Ratcheting strain in interstitial free steel, Mater. Sci. Eng. A 575 (2013) 127–135.
- [5] A. Sarkar, B.K. Kumawat, J.K. Chakravarty, Ratcheting behavior of 20MnMoNi55 reactor pressure vessel steel, J. Nucl. Mater. 467 (2015) 500–504.
- [6] S.K. Paul, S. Sivaprasad, S. Dhar, S. Tarafder, Ratcheting and low cycle fatigue behavior of SA333 steel and their life prediction, J. Nucl. Mater. 401 (2010) 17–24.
- [7] G.R. Ahmadzadeh, A. Varvani-Farahani, Triphasic ratcheting strain prediction of materials over stress cycles, Fatigue Fract. Eng. Mater. Struct. 35 (2012) 929–935.
- [8] G. Kang, Y. Liu, Uniaxial ratcheting and low-cycle fatigue failure of the steel with cyclic stabilizing or softening feature, Mater. Sci. Eng. A 472 (2008) 258–268.
- [9] G. Kang, Q. Gao, X. Yang, Uniaxial cyclic ratcheting and plastic flow properties of SS304 stainless steel at room and elevated temperatures, Mech. Mater. 34 (2002) 145–159.
- [10] K.K. Ray, K. Dutta, S. Shivaprasad, S. Tarafder, Fatigue damage of AISI 304LN stainless steel: role of mean stress, Procedia Eng. 2 (2010) 1805–1813.
- [11] I. Ben Naceur, K. Saï, T. Hassan, G. Cailletaud, Micromechanical modeling of the ratcheting behavior of 304 stainless steel, J. Eng. Mater. Trans. ASME 2 (2016) 138–147.
- [12] G. Kang, Y. Liu, Y. Dong, Q. Gao, Uniaxial ratcheting behaviors of metals with different crystal structures or values of fault energy: macroscopic experiments, J. Mater. Sci. Technol. 27 (2011) 453–459.
- [13] G. Kang, Q. Gao, L. Cai, X. Yang, Y. Sun, Experimental study on uniaxial and multiaxial strain cyclic characteristic and ratcheting of 316 stainless steel, J. Mater. Sci. Technol. 17 (2001) 219–223.
- [14] G. Cailletaud, K. Saï, A polycrystalline model for the description of ratcheting: effect of intergranular and intragranular hardening, Mater. Sci. Eng. A 480 (2008) 24–39.
- [15] D. Abdeljaoued, I. Ben Naceur, K. Saï, G. Cailletaud, A new polycrystalline plasticity model to improve ratcheting strain prediction, Mech. Res. Commun. 36 (2009) 309–315.
- [16] S. Kwofie, H.D. Chandler, Low cycle fatigue under tensile mean stresses where cyclic life extension occurs, Int. J. Fatigue 23 (2001) 341–345.
- [17] J. Ding, G. Kang, Q. Kan, Y. Liu, Constitutive model for uniaxial time-dependent ratcheting of 6061-T6 aluminum alloy, Comput. Mater. Sci. 57 (2012) 67–72.
- [18] G.R. Ahmadzadeh, A. Varvani-Farahani, Concurrent ratcheting-fatigue damage analysis of uniaxially loaded A-516 Gr.70 and 42CrMo steels, Fatigue Fract. Eng. Mater. Struct. 35 (2012) 962–970.
- [19] A. Varvani-Farahani, Fatigue-ratcheting damage assessment of steel samples under asymmetric multiaxial stress cycles, Theor. Appl. Fract. Mech. 73 (2014) 152–160.